

## Article

# Experimental Study on Strength and Microstructure of Glacial Till Stabilized by Ionic Soil Stabilizer

Yifan Huang <sup>1,2,\*</sup> , Wenfeng Fan <sup>3</sup>, Jinliang Wu <sup>1,4</sup>, Xinglong Xiang <sup>1</sup> and Guan Wang <sup>4</sup><sup>1</sup> School of Civil Engineering, Chongqing Jiaotong University, Chongqing 400074, China<sup>2</sup> National and Local Joint Engineering Laboratory of Traffic Civil Engineering Materials, School of Civil Engineering, Chongqing Jiaotong University, Chongqing 400074, China<sup>3</sup> Chongqing Zhixiang Paving Technology Engineering Co., Ltd., China Merchants Chongqing Communications Technology Research and Design Institute, Chongqing 401336, China<sup>4</sup> Chongqing Jiaoda Construction Engineering Quality Test Center Co., Ltd., Chongqing Jiaotong University, Chongqing 400074, China

\* Correspondence: 622200951088@mails.cqjtu.edu.cn; Tel.: +86-132-2029-8089

**Abstract:** Glacial till, widely distributed in southwest China, is a special soil directly deposited by detritus formed from melting Quaternary glaciers. In this paper, the F1 ionic soil stabilizer was adopted for stabilizing the glacial till to improve its mechanical strength. A series of micro and macro tests were carried out to study the mechanical properties and microstructure of stabilized soil with the F1 ionic soil stabilizer. The results show that the F1 ionic soil stabilizer can destroy the diffuse double layer structure on the surface of glacial till particles and reduce the thickness of the adsorbed water layer through strong cation exchange and hydrophobic interactions of active sulfonated oil, which reduce the spacing of glacial till particles, enhance the aggregation of glacial till particles, and effectively suppress the swelling deformation of the glacial till. It can be concluded that the water sensitivity and compaction characteristics of glacial till can be significantly improved by the stabilization of the F1 ionic soil stabilizer. Moreover, the mechanical strength of the glacial till can be significantly improved by the stabilization of the F1 ionic soil stabilizer. This article is helpful as a guideline for practical design and future research on applying the F1 ionic soil stabilizer to improve the bearing capacity of foundations in glacial till areas.

**Keywords:** glacial till; ionic soil stabilizer; strength characteristics; stabilization mechanism; microstructural



**Citation:** Huang, Y.; Fan, W.; Wu, J.; Xiang, X.; Wang, G. Experimental Study on Strength and Microstructure of Glacial Till Stabilized by Ionic Soil Stabilizer. *Buildings* **2022**, *12*, 1446. <https://doi.org/10.3390/buildings12091446>

Academic Editor: Abdelhafid Khelidj

Received: 21 August 2022

Accepted: 11 September 2022

Published: 14 September 2022

**Publisher's Note:** MDPI stays neutral with regard to jurisdictional claims in published maps and institutional affiliations.



**Copyright:** © 2022 by the authors. Licensee MDPI, Basel, Switzerland. This article is an open access article distributed under the terms and conditions of the Creative Commons Attribution (CC BY) license (<https://creativecommons.org/licenses/by/4.0/>).

## 1. Introduction

Glacial till is a particular soil caused by glacial movement and accumulated through reconstruction movements such as landslides and debris flows. The glacial till formed in the Quaternary Pleistocene is widely distributed in southwest China [1,2]. Glacial till can not be directly used as subgrade filler because of its distinctive properties formed by the particular formation environment and process, such as high porosity, high moisture content, low bearing capacity, and strong water sensitivity [3–5]. Discarding the glacial till and replacing it with other fillers will significantly increase transportation and construction costs [6]. Therefore, glacial till with complex engineering properties usually needs to be stabilized by physical and chemical methods to improve its mechanical strength [7–10].

Portland cement is one of the most widely used soil stabilizers, providing an efficient soil solidification effect [11–13]. A large amount of cement injected into the soil will cause soil pollution. In addition, in the context of global warming, the Portland cement production process consumes a lot of resources and energy and emits a multitude of greenhouse gases and pollutants [14–17]. Finding environmentally friendly and sustainable alternatives to Portland cement is crucial to reducing carbon emissions and environmental pollution. Recent studies have shown that industrial wastes and by-products such as fly ash [18,19],

slag [20,21], lime [22,23], waste glass [24], red mud [25], blast furnace slag [26], and cement kiln dust [27] can substitute cement for cement soil stabilization. Nevertheless, traditional soil stabilizers such as cement, lime, and fly ash still have disadvantages such as high cost and long construction.

With the advancement of materials science and the need for engineering construction, ionic soil stabilizers have received extensive attention as non-traditional soil stabilizers [28–30]. Unlike traditional soil stabilizers such as lime, cement, and fly ash, ionic soil stabilizers (ISS) can reduce environmental pollution and process costs and shorten construction periods [31]. ISS mainly destroys the diffuse double layer structure of clay particles and reduces the adsorption force of clay particles to water, thereby enhancing the aggregation of the clay particles [32–34]. Currently, ISS has been effectively applied in red clay [35–39], frozen soil [40,41], bentonite [42,43], clay [44,45], expansive soil [46], loess [47], and shale soil [48]. However, there are few studies on stabilizing glacial till by ISS, and the mechanical properties and microstructure of stabilized glacial till need to be further explored.

In this paper, the F1 ionic soil stabilizer (F1) was used to stabilize the glacial till in southwest China. The influence of F1 on the fundamental physical properties, mechanical strength, and microstructure of the glacial till was studied by Atterberg limits, compaction, California bearing ratio (CBR), and unconfined compressive strength (UCS) tests. The stabilization mechanism of F1 and the difference in the microstructure between F1 stabilized glacial till and natural glacial till were studied by scanning electron microscopy (SEM) and X-ray diffraction (XRD). These research results will help in the practical application of glacial till in subgrade construction and hope to provide a valuable reference for applying and promoting ionic soil stabilizers in glacial till areas.

## 2. Materials and Methods

### 2.1. Materials

#### 2.1.1. F1 Ionic Soil Stabilizer

FORMULA F1 ionic soil stabilizer (F1) is mainly composed of acrylic acid sulfonated polymer. It is a faint yellow pure solution with a pungent odor at room temperature and is easily soluble in water. Its density is  $1.35 \text{ g/cm}^3$ . F1 must be diluted with water in a certain proportion before testing and engineering application. In this paper, the dilution ratio is 1:200 [46,49,50]. The basic requirements for the soil treated with F1 are that the pH value of the soil is less than 8, and the plasticity index of the soil is greater than or equal to 10.

#### 2.1.2. Glacial Till

The glacial till, formed in the Middle Pleistocene of the Quaternary, was taken from Leshan City, Sichuan Province, China, as shown in Figure 1. Its natural density is in the range of  $1.9$  to  $2.2 \text{ g/cm}^3$ . The natural density of glacial till increases with the increase in compactness, and the natural density decreases with the decrease in soil particle size.



**Figure 1.** Glacial till. (a) Field sampling point of glacial till. (b) Laboratory sample of glacial till.

Glacial till is weakly acidic (pH = 6.1), and its plasticity index is 18.3. Therefore, its parameters meet the requirements of F1 for soil. The particle size analysis test was carried out in accordance with Standard JTG 3430-2020 [51]. The grain size distribution curve of the glacial till is presented in Figure 2, and the grain size distribution indexes are summarized in Table 1.

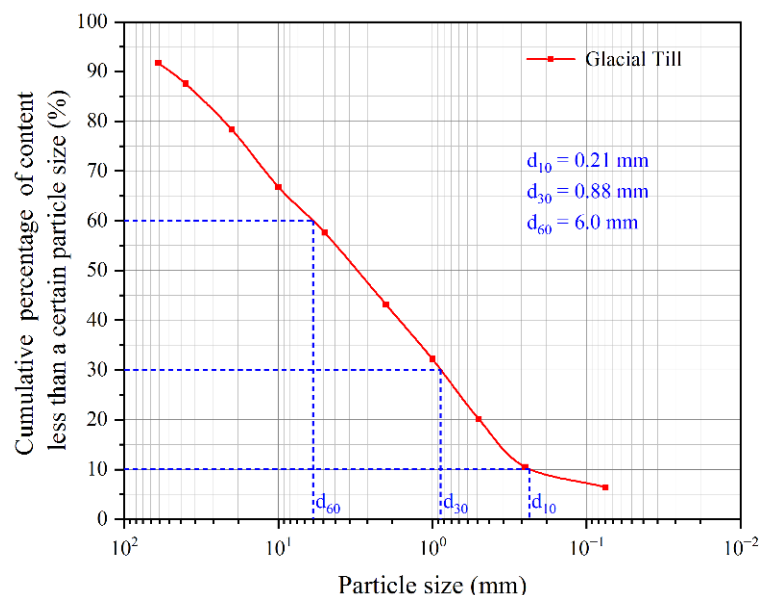


Figure 2. Grain size distribution curve.

Table 1. This is a table. Tables should be placed in the main text near to the first time they are cited.

Effective Grain Size (mm)	Median Grain Size (mm)	Constrained Grain Size (mm)	Coefficient of Uniformity	Coefficient of Curvature
0.21	0.88	6.0	28.57	0.61

The mass ratio (mass of the component/mass of the sample) of the giant-grained component (>60 mm) in the glacial till sample is 8.27%, which is less than 15%. Meanwhile, the mass ratio of the coarse-grained component (0.075 mm–60 mm) is 81.18%, which is more than 50%. Therefore, the glacial till is determined to be coarse-grained soil. The mass ratio of the sand component is 36.77%, which is less than 48.55% of the mass ratio of the gravel component. Moreover, the mass ratio of the fine-grained component (<0.075 mm) is 6.41%, which is greater than 5%. Therefore, the glacial till sample is determined to be fine-grained gravelly soil.

### 2.1.3. Sample Preparation

F1 concentrations for stabilizing glacial till were 0.20 L/m<sup>3</sup>, 0.25 L/m<sup>3</sup>, 0.30 L/m<sup>3</sup>, 0.35 L/m<sup>3</sup> and 0.40 L/m<sup>3</sup>, and 0.20 L/m<sup>3</sup> means that every 1 m<sup>3</sup> soil is doped with 0.2 L F1. F1 was diluted with water and sprayed evenly on the surface of the glacial till. Additional water can be added if needed. Afterward, the samples were squeezed and stirred by hand for 10–15 min to thoroughly mix F1 into the glacial till. The glacial till after F1 treatment was put into a closed container and soaked in F1 solution for three days. Lastly, the samples were spread outdoors until they dried naturally.

## 2.2. Methods

In order to study the effect of F1 on the basic physical and mechanical properties and microstructure of the glacial till, the Atterberg limits, compaction, CBR, UCS, SEM, and XRD tests were carried out on the glacial till before and after stabilization.

### 2.2.1. Physical Properties Tests

The Atterberg limits and compaction tests were carried out on the glacial till before and after stabilization with F1 following Standard JTG 3430-2020 [51]. Thereby, the liquid limit, plastic limit, optimum moisture content, and maximum dry density of the glacial till with F1 of different concentrations were obtained.

### 2.2.2. Mechanical Properties Tests

The CBR test was carried out on the glacial till before and after stabilization with F1 following Standard JTG 3430-2020 [51]. The test adopts the compaction molding method, with 30 times, 50 times, and 98 times of compaction, respectively. After that, the bearing plates were placed on the samples, and the samples were soaked in water for 48 h. The water swelling and penetration tests were performed on the samples with different compaction times.

For the UCS test, the glacial till before and after stabilization with F1 was made as cylindrical samples with a size of  $\phi$  100 mm  $\times$  100 mm. The samples were static pressure formed with a press, and the compaction degree of the sample was controlled to be 96%. After that, the samples were put into plastic boxes and sealed. Then the plastic boxes were immediately put into a standard curing box with a humidity of 95% and a temperature of  $20 \pm 2$  °C. The UCS of the glacial till and the stabilized soil doped with different concentrations of F1 after curing for 7 days, 14 days, and 28 days were tested following Standard JTG 3430-2020 [51], respectively.

### 2.2.3. Microstructure Tests

The glacial till and F1 solidified soil microstructures were analyzed by ZEISS Sigma 300 scanning electron microscope and SmartLab 9 kw X-ray diffractometer.

## 3. Results

### 3.1. Effects of F1 on Atterberg Limits

The plastic limit, liquid limit, and plastic index of the glacial till with different concentrations of F1 are shown in Figure 3. Compared with the glacial till, the liquid limit, plastic limit, and plasticity index of F1 stabilized soil decreased. When the concentration of F1 was  $0.35 \text{ L/m}^3$ , the liquid limit, plastic limit, and plasticity index were the minimum. The liquid limit decreased from 46.6% to 40.1%, a decrease of 13.9%; the plastic limit decreased from 28.3% to 24.5%, a decrease of 13.4%; the plasticity index also decreased from 18.3 to 15.5, a decrease of 15.3%. However, the liquid limit, plastic limit, and plastic index increased slightly when concentration of F1 exceeded  $0.35 \text{ L/m}^3$ .

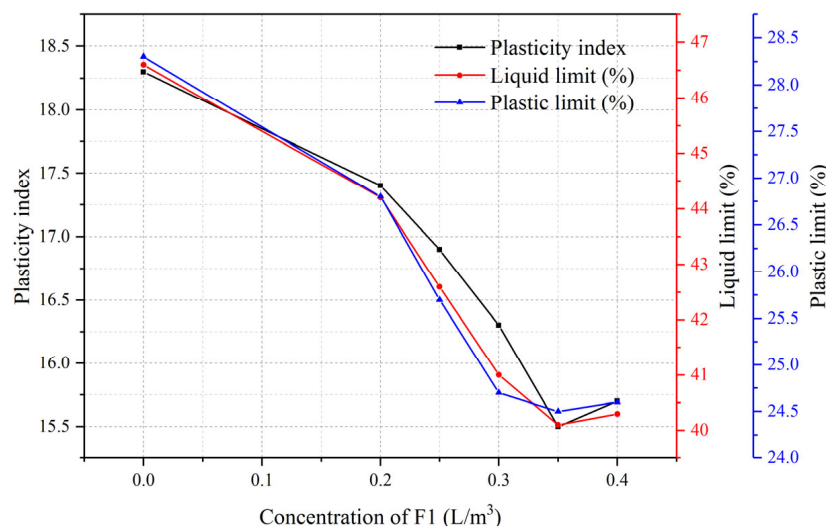


**Figure 3.** The relationship between concentration of F1 and Atterberg limits.

F1 provided many strong cations, which reacted with the anions on the surface of the glacial till particles and replaced the cations and polar water molecules with weak adsorption. The above resulted in a reduction in diffuse double layer and adsorbed water layer thickness. Therefore, the liquid limit, plastic limit, and plastic index of the glacial till were reduced, which proved that F1 reduced the water sensitivity of the glacial till. Furthermore, when the concentration of F1 exceeded  $0.35 \text{ L/m}^3$ , the influence of F1 on the liquid limit and plastic limit of glacial till was reduced, and the strong cations provided by F1 were nearly saturated.

### 3.2. Effects of F1 on Maximum Dry Density and Optimum Moisture Content

The compaction test showed differences in the optimum moisture content and maximum dry density between the stabilized soils with different concentrations of F1. The compaction test results of glacial till doped with different concentrations of F1 are shown in Figure 4 and Table 2.

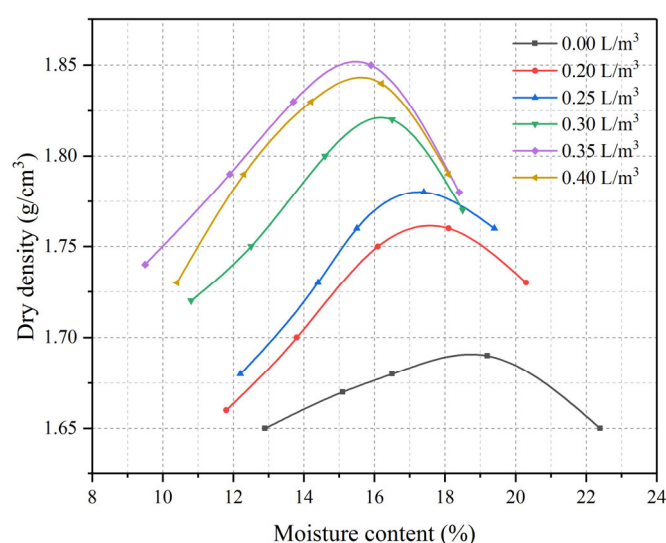


Figure 4. Moisture–density curve.

Table 2. Compaction test results.

Concentration of F1 (L/m³)	Maximum Dry Density (g/cm³)	Optimum Moisture Content (%)
0	1.69	18.6
0.2	1.76	17.8
0.25	1.78	17.4
0.30	1.82	16.5
0.35	1.85	15.1
0.40	1.83	15.6

The maximum dry density of stabilized soil increased with increased concentration of F1, and the optimum water content of stabilized soil decreased with increased concentration of F1. When the concentration of F1 was  $0.35 \text{ L/m}^3$ , the maximum dry density of the stabilized soil reached a maximum of  $1.85 \text{ g/cm}^3$ , an increase of 9.5%; and the optimum moisture content of the stabilized soil reached a minimum of 15.1%, a decrease of 18.8%. However, when the concentration of F1 exceeded  $0.35 \text{ L/m}^3$ , the maximum dry density of the glacial till decreased slightly, and the optimum moisture content of the glacial till increased slightly.

Due to the strong cations rapidly dissociated from the F1 solution, the cation exchange occurred on the surface of the glacial till particles, which contributed to changes in the internal pores of the soil and prevented water molecules from being adsorbed by the glacial



till particles. Therefore, part of the free water in the glacial till was removed during the compaction process, and the soil reached greater compactness with the same compaction effort. The strong cation provided by F1 reacted irreversibly with the surface of glacial till particles when F1 was fully integrated into the glacial till. When the concentration of F1 exceeded  $0.35 \text{ L/m}^3$ , F1 dissociated excessive strong cations, which generated charge repulsion force with the cations on the surface of the glacial till particles to increase the spacing of the glacial till particles. It resulted in a decrease in the maximum dry density of the glacial till while increasing the optimum moisture content of the glacial till.

### 3.3. Effects of F1 on CBR

The CBR test results of the glacial till with different numbers of hits and different concentrations of F1 are shown in Figure 5. The CBR of the glacial till with different concentrations of F1 increased with the number of hits. Nevertheless, the degree of increase was different. Among them, the CBR of the glacial till without F1 increased slowly with the number of hits, and the CBR of the F1 stabilized soil increased rapidly with the number of hits. It can be seen that the number of hits played an important influence on the CBR of the glacial till. Because the degree of compaction of the soil increased with the number of hits. Therefore, the frictional resistance on the surface of glacial till particles increased, which led to the enhancement of the ability of soil to resist local shear deformation and the increase in CBR.

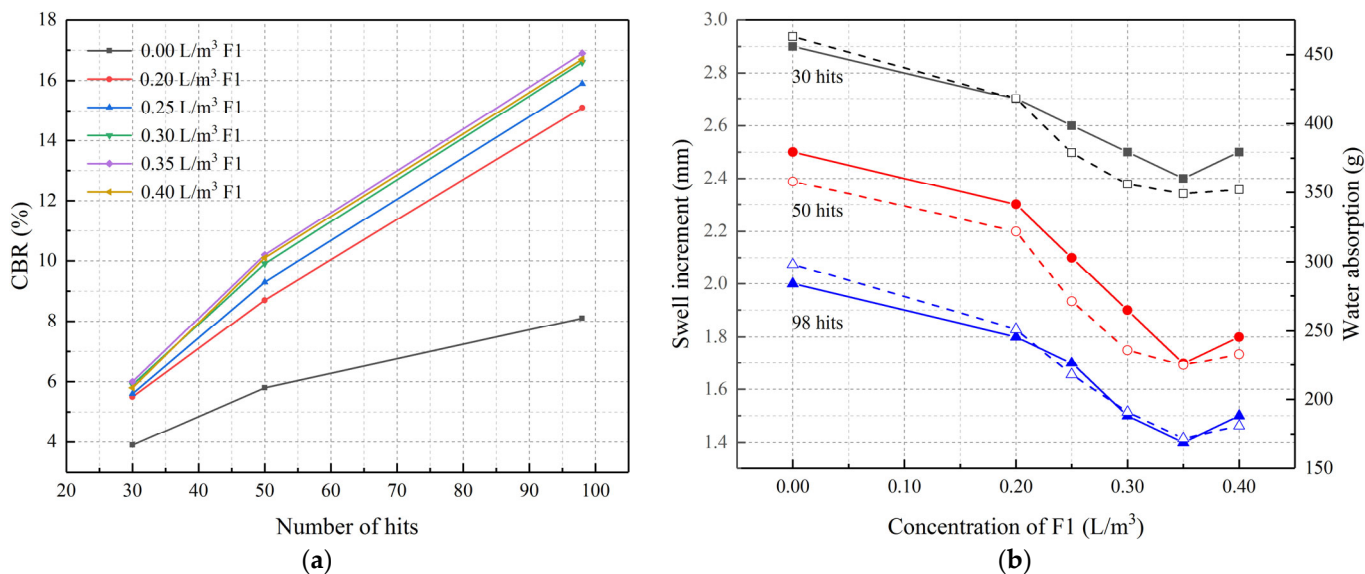


**Figure 5.** CBR test results. (a) The relationship between CBR and the number of hits; (b) the relationship between the concentration of F1 and swell increment/water absorption.

It can be seen from Figure 5a that the CBR of stabilized soil increased with the concentration of F1. When the concentration of F1 was  $0.35 \text{ L/m}^3$ , and the number of hits was 98, the CBR reached a maximum of 16.9%, which is 108.6% higher than that of the glacial till without F1. When the concentration of F1 exceeded  $0.35 \text{ L/m}^3$ , the CBR of stabilized soil decreased slightly. F1 reduced the adsorbed water layer thickness of the glacial till particles and increased the compactness of the glacial till. Therefore, the bearing capacity of the glacial till is improved.

It can be seen from Figure 5b that the expansion and water absorption of the glacial till decrease with the increase in F1 concentration. With the 98 hits and F1 concentration of  $0.35 \text{ L/m}^3$ , the swell increment and water absorption of the glacial till reached the minimum, 1.4 mm and 172 g, which were 41.7% and 51.7% higher than those of glacial till without F1. However, the swell increment and water absorption of the glacial till increased slightly when the concentration of F1 exceeded  $0.35 \text{ L/m}^3$ . It was verified that F1

prevented the adsorption of water by the glacial till particles through the ion exchange and the hydrophobic interaction of sulfonated oil, which improved the water stability of the glacial till.

### 3.4. Effects of F1 on UCS

In stabilized soil engineering, the UCS with a curing age of 7 days is often used as a reference to determine the optimal concentration of F1. As shown in Figure 6, the sample disintegrated or cracked after the glacial till was cured for six days and then immersed in water for 5 h. It showed that the water stability of the glacial till was poor. Moreover, although the water stability of the glacial till with the addition of F1 enhanced, it was also damaged to a certain extent. Therefore, the UCS tests were carried out on unsaturated samples with curing ages of 7 days, 14 days, and 28 days. The test results are shown in Figure 7.

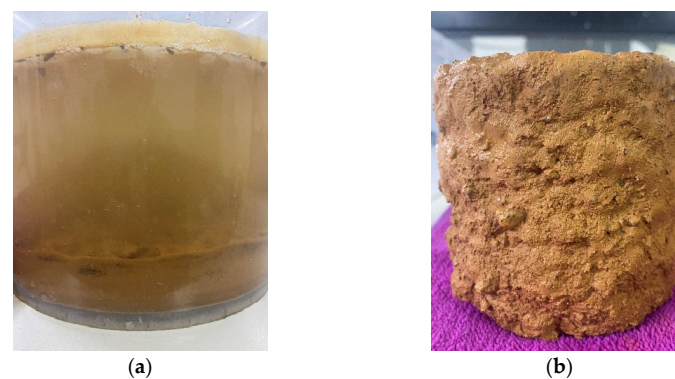


**Figure 6.** State of the sample after curing for 6 days and immersion for 5 h. (a) Glacial till without F1; (b) stabilized soil doped with F1 at a concentration of 0.35 L/m<sup>3</sup>.

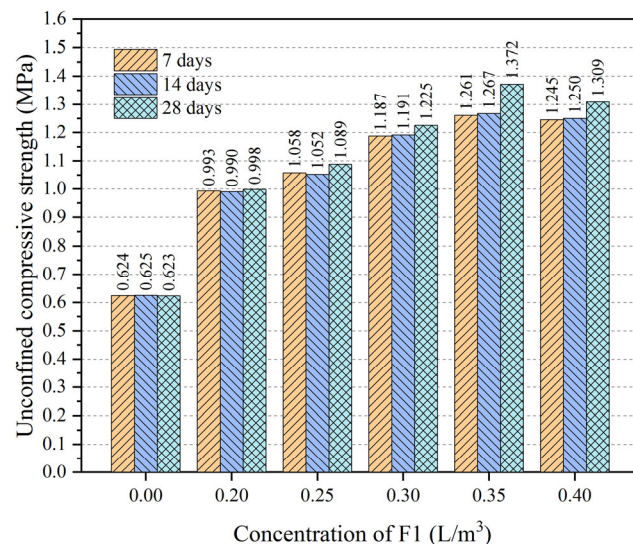


**Figure 7.** UCS of glacial till with different concentrations of F1 and different curing ages.

It can be seen from Figure 7 that the addition of F1 effectively improved the UCS of the glacial till. The UCS of stabilized soil mixed with different concentrations of F1 at 7 days increased by 59.1%, 69.6%, 90.2%, 102.1%, and 99.5%, respectively, compared with the glacial till in an unsaturated state. When the concentration of F1 is 0.35 L/m<sup>3</sup>, the UCS of stabilized soil reaches a maximum of 1.261 MPa. The UCS of the glacial till did not change with the curing age. The UCS of F1 stabilized soil with curing ages of 7 days and 14 days did not change significantly. The UCS of the F1 stabilized soil with a curing age of

28 days only increased slightly, and the UCS of stabilized soil with an F1 concentration of  $0.35 \text{ L/m}^3$  is  $1.372 \text{ Mpa}$ , which is 8.8% higher than the UCS at seven days. Therefore, F1 significantly strengthened the glacial till, and the curing age had little effect on the UCS of the stabilized soil.

### 3.5. Microstructural Analysis

ZEISS Sigma 300 scanning electron microscope was used to observe the surface morphology and structure of glacial till and stabilized soil with an F1 concentration of  $0.35 \text{ L/m}^3$  at 2000 times, 5000 times, 10,000 times, and 20,000 times magnification. The scanning electron micrographs were then analyzed using MIPAR image processing software. Figure 8 is the scanning electron micrographs processed by MIPAR software, in which red and gray represent pore and soil skeleton structure, respectively.

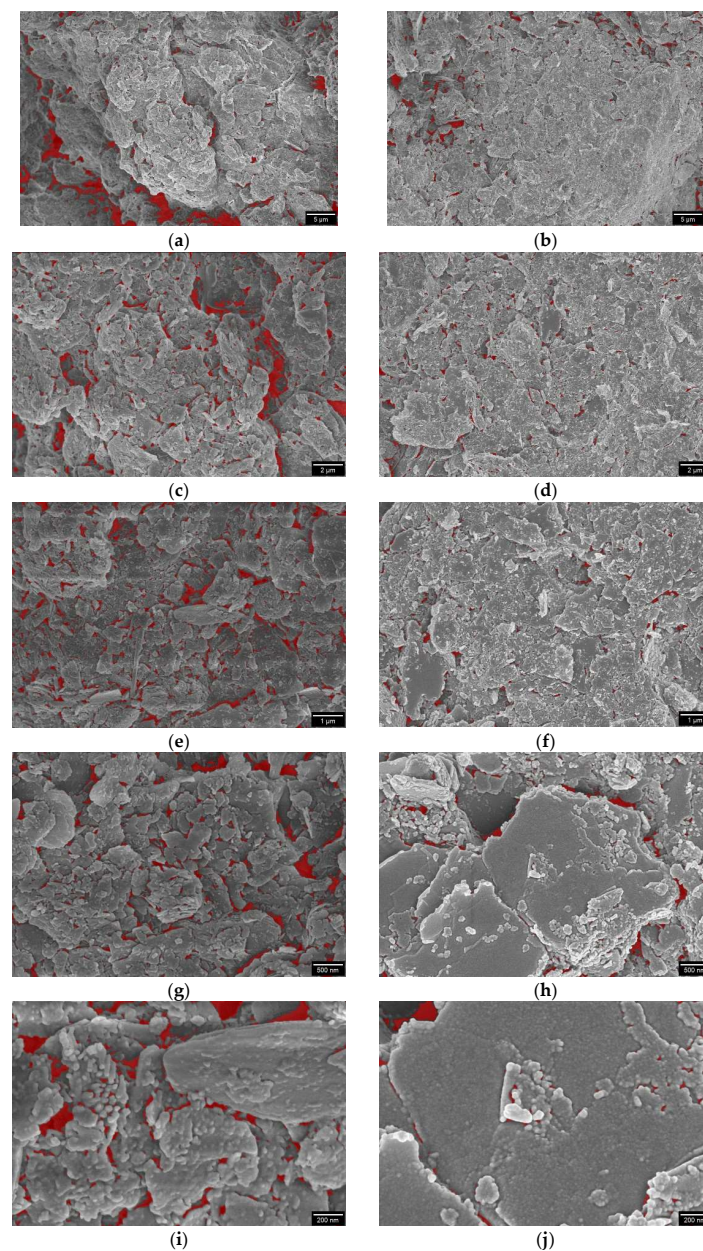


**Figure 8.** Scanning electron micrographs. (a)  $2000 \times$  glacial till; (b)  $2000 \times$   $0.35 \text{ L/m}^3$  F1 stabilized soil; (c)  $5000 \times$  glacial till; (d)  $5000 \times$   $0.35 \text{ L/m}^3$  F1 stabilized soil; (e)  $10,000 \times$  glacial till; (f)  $10,000 \times$   $0.35 \text{ L/m}^3$  F1 stabilized soil; (g)  $20,000 \times$  glacial till; (h)  $20,000 \times$   $0.35 \text{ L/m}^3$  F1 stabilized soil; (i)  $50,000 \times$  glacial till; (j)  $50,000 \times$   $0.35 \text{ L/m}^3$  F1 stabilized soil.



It can be seen from scanning electron micrographs (Figure 9) that the microstructures of the glacial till before and after the incorporation of F1 had apparent changes. Glacial till particles with a 7-day curing age were piled up disorderly, their combinations were not tight, and some soil particles were needle-like. There were large voids between the clods formed by stacking soil particles, accompanied by open structures. The number of needle-like soil particles was significantly reduced in the F1 stabilized soil samples cured for 7 days. The fine particles and needle-like particles originally existing in the glacial till were stacked to form large particles in the form of flakes and agglomerates, and the soil particles were more closely combined. Moreover, the soil particles formed by stacking had larger particle sizes and smoother surfaces, and the structural units were mainly in the form of surface-surface contact. The voids between the clods formed by stacking soil particles were smaller than that of the glacial till without F1. Consequently, F1 reduced the pore sizes of the glacial till.

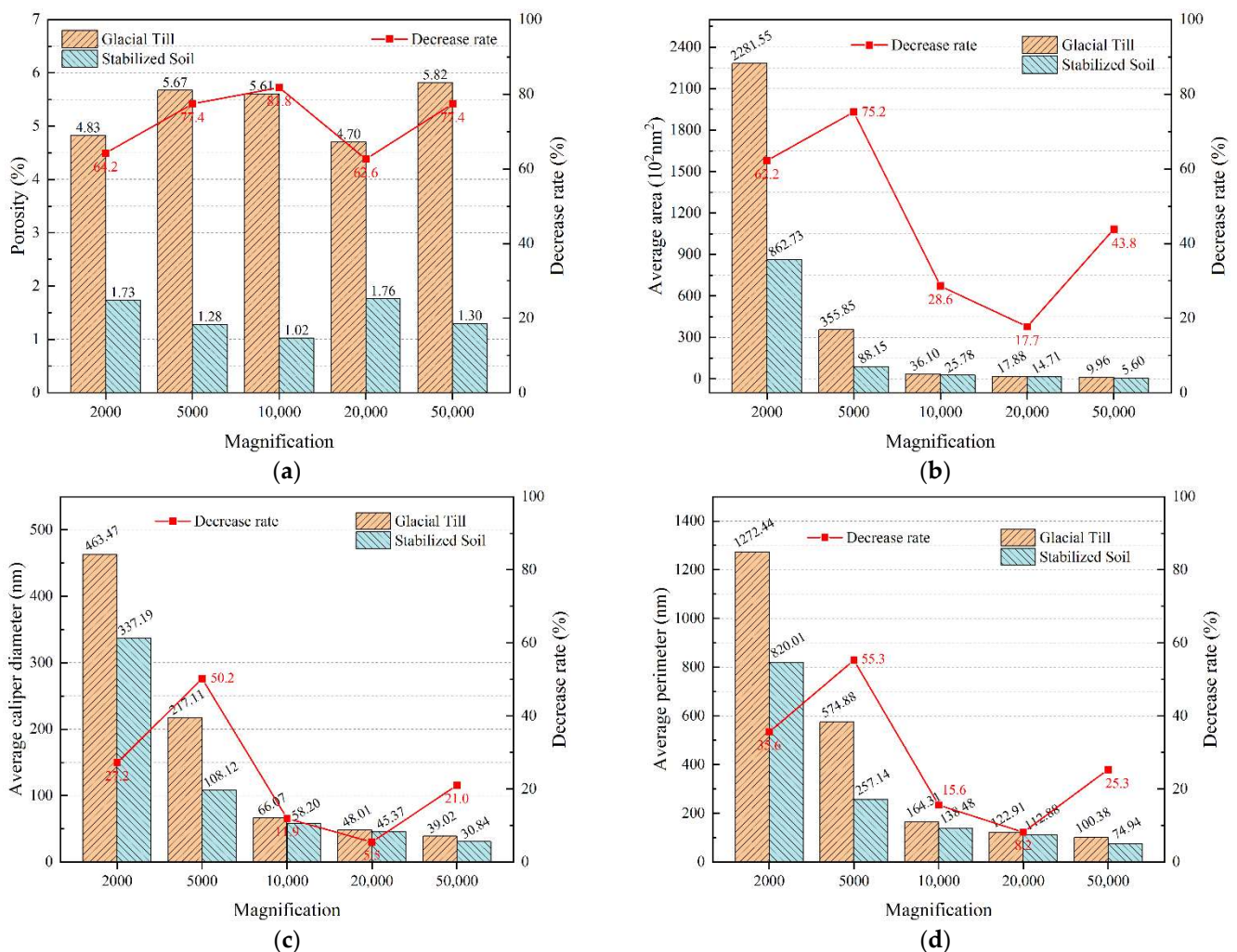


**Figure 9.** Pore structure parameters of glacial till and stabilized soil. (a) Porosity; (b) average pore area; (c) average pore caliper diameter; (d) average pore perimeter.

The MIPAR image processing software was used to identify and extract the porosities, pore areas, caliper diameters, and perimeters of the glacial till and stabilized soil with an F1 concentration of  $0.35 \text{ L/m}^3$ . The ratio of the pore area to the picture area is defined as porosity. It can be seen from Figure 10 that the porosities, average pore areas, average pore caliper diameters, and average pore perimeters were reduced in the stabilized soil compared with the glacial till. F1 made the glacial till particles combine more closely and

effectively reduced the number of pores by reducing the thickness of the adsorbed water layer of the glacial till particles. Moreover, F1 effectively reduced the pore size of the glacial till, which turned macropores and mesopores into micropores.

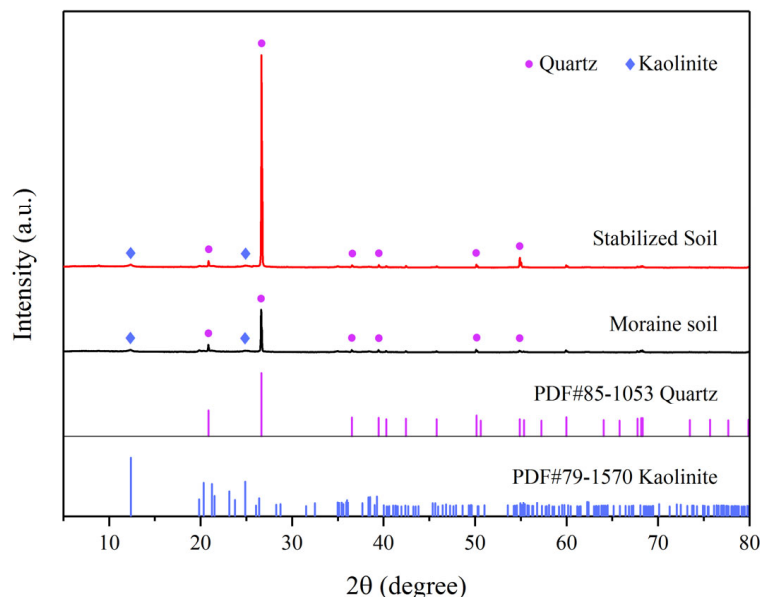


**Figure 10.** X-ray diffraction patterns of glacial till and stabilized soil.

In order to explore the changes in mineral compositions in glacial till before and after F1 stabilization, XRD tests were carried out on natural glacial till and stabilized soil with an F1 concentration of  $0.35 \text{ L/m}^3$ . Based on XRD data, MDI jade software was used to analyze mineral compositions and interplanar spacings [52]. The test results are shown in Figure 10 and Table 3.

**Table 3.** Mineral interplanar spacings of glacial till and stabilized soil.

2θ (Degree)	Interplanar Spacing (nm)	
	Glacial Till	Stabilized Soil
20	4.4712	4.4625
40	2.2373	2.2361
60	1.5420	1.5414

It can be known that the main mineral compositions of glacial till and F1 stabilized soil were quartz and kaolinite from the characteristic curve and eigenvalue of the XRD pattern. No new mineral diffraction peaks appeared in the stabilized soil samples. Therefore, no new mineral compositions were generated in the stabilized soil with the addition of F1. The mineral interplanar spacings of the glacial till and the stabilized soil were extracted with angles of incidence ( $2\theta$ ) were  $20^\circ$ ,  $40^\circ$ , and  $60^\circ$ , as shown in Table 3. At the same angle, the interplanar spacings of the F1 stabilized soil are less than that of the natural glacial till in low-angle and high-angle areas. From a microscopic perspective, F1 reduced the spacings between the glacial till particles, thereby improving the compactness of the glacial till.

#### 4. Discussion

It is verified that F1, as a new type of ionic soil stabilizer, improved the physical and mechanical properties of glacial till through a series of micro and macro tests. Combined with the stabilization mechanism and properties of ionic soil stabilizers, the stabilization mechanism of F1 on glacial till was analyzed.

#### 4.1. Strong Cation Exchange

The addition of F1 affects the diffuse double layer structure on the surface of the glacial till particles [34]. Negative charges on the surface of the glacial till particles generate an electric field near the glacial till particles. A large number of cations are adsorbed around glacial till particles by electrostatic attraction. The cation content decreases with the increased distance from the surface of glacial till particles. Therefore, most cations are located closest to the surface of the glacial till particles. High-valence cations can replace low-valence cations. The cation with a smaller hydration radius has larger exchange potential energy. F1 rapidly dissociates strong cations ( $\text{H}_3\text{O}^+$ ) when encountering water. The hydration radius of  $\text{H}_3\text{O}^+$  is much smaller than that of the cations on the surface of the glacial till. Therefore, it can undergo cation exchange reactions with cations on the surface of glacial till particles and polar water molecules with weak connections [49]. When the F1 aqueous solution is added to the glacial till, the strong cations provided by F1 increase the ion concentration on the surface of the glacial till.  $\text{H}_3\text{O}^+$  first bonds to vacancy anions on the surface of glacial till particles.  $\text{H}_3\text{O}^+$  then exchanges with cations on the surface of the glacial till particles. The bonding between glacial till particles and water molecules is broken so that the adsorbed water in the diffuse double layer structure is released. The cations in the diffuse double layer structure penetrate into the solution with increasing ion concentration [53]. Therefore, F1 reduces the electric potential of the glacial till particles, destroys the diffuse double layer structure, and reduces the thickness of the adsorbed water layer, which reduces the water absorption by the glacial till and enhances the attraction between glacial till particles. The reaction between F1 and glacial till is irreversible, and the dissociated cations are adsorbed on the surface of glacial till particles and cannot be replaced. After mechanical compaction, the water in the glacial till will be squeezed out, resulting in a denser soil structure. The mechanism is shown in Figure 11.

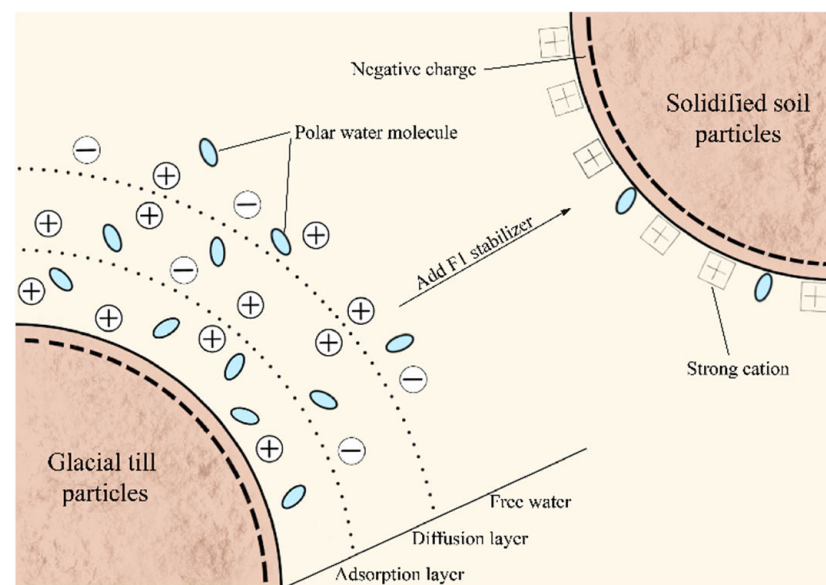


**Figure 11.** Schematic diagram of cation exchange.

Based on the above test results, F1 increased the maximum dry density of the glacial till while reducing the optimum water content of the glacial till by strong cation exchange, thereby increasing the mechanical strength of the glacial till. However, when the concentration of F1 exceeds a certain value, the strong cations bound on the surface of the glacial till particles generate charge repulsion force with the excessive strong cations dissociated from F1, which increases the distances between the glacial till particles. It results in a decrease in the maximum dry density of the glacial till and an increase in the optimum moisture content of the glacial till, thereby reducing the mechanical strength of the glacial till.

#### 4.2. Hydrophobic Interaction

F1 contains active sulfonated oils, consisting of a hydrophilic head and a hydrophobic tail [35]. After the hydrophilic headgroups are dissociated, they can bond with metal cations on the surface of glacial till particles to form chemical looping, which occupies a cationic vacancy on the surface of glacial till particles. The hydrophilic headgroups are dissolved in the adsorbed water on the surface of the glacial till particles and adsorbed on the surface of the glacial till particles. Moreover, the hydrophobic tails form a hydrophobic oil layer on the surface of the glacial till particles due to their characteristics, which block the entry of water molecules. The presence of chemical looping and oily layers makes it easy for internal water to drain out and difficult for external water to enter. The combined effect of the hydrophilic headgroups and the hydrophobic tails reduces the thickness of the adsorbed water layer of the glacial till particles. Therefore, F1 can reduce the water adsorption capacity of glacial till to improve its compactness. The mechanism is shown in Figure 12.

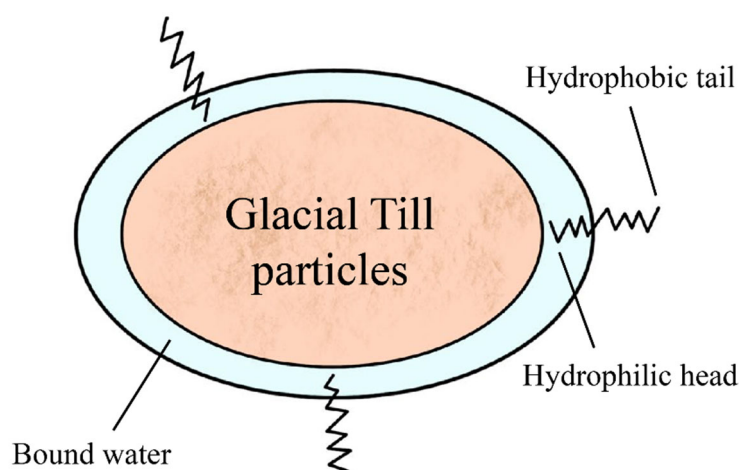


Figure 12. Schematic diagram of cation exchange.

#### 5. Conclusions

The physical parameters, mechanical properties, and microstructures were analyzed through the Atterberg limits test, geotechnical compaction test, CBR test, UCS test, SEM, and XRD test. The effect and mechanism of the F1 in stabilizing glacial till were studied. The research conclusions are as follows:

1. F1 can reduce the liquid limit, plastic limit, plastic index, and optimum moisture content of the glacial till and increase the maximum dry density of the glacial till, which significantly improves the water sensitivity and compaction characteristics of the glacial till.
2. F1 can significantly increase the CBR and UCS of the glacial till and effectively restrain its swelling deformation.  $0.35 \text{ L/m}^3$  is the optimum concentration of F1 for stabilizing glacial till. Compared with the natural glacial till, the stabilized soil with an F1 concentration of  $0.35 \text{ L/m}^3$  increases the CBR by 108.6%, and the UCS increases by 102.1%.
3. F1 can accumulate the fine particles and needle-like particles of the glacial till into large particles in the form of flakes and agglomerates, which significantly reduces the porosity and pore sizes of the glacial till, thereby increasing the compactness of the glacial till. F1 can reduce the interplanar spacing of the glacial till, and the mineral composition does not change during the stabilization process.
4. F1 can destroy the diffuse double layer structure on the surface of glacial till particles and reduce the thickness of the adsorbed water layer through strong cation exchange and hydrophobic interactions of active sulfonated oil, which reduce the spacing of glacial till particles, enhance the aggregation of glacial till particles. After the F1 stabi-



lized soil was compacted, the soil particles formed a layered stacking structure with more compact arrangements and larger agglomerates, enhancing the compactness of the glacial till.

5. Compared with lime, cement, and other traditional soil stabilizers, F1 has many advantages, such as simple construction, low cost, short maintenance period, and environmental friendliness. Therefore, it has broad application prospects in soil improvement and road construction in glacial till areas.

**Author Contributions:** Conceptualization, Y.H. and W.F.; Data curation, W.F.; Formal analysis, Y.H. and W.F.; Funding acquisition, J.W.; Investigation, X.X. and G.W.; Methodology, Y.H., W.F. and J.W.; Validation, Y.H. and J.W.; Project administration, J.W.; Resources, X.X. and G.W.; Supervision, J.W.; Writing—original draft, Y.H.; Writing—review and editing, Y.H. and W.F. All authors have read and agreed to the published version of the manuscript.

**Funding:** This research received no external funding.

**Informed Consent Statement:** Informed consent was obtained from all subjects involved in the study.

**Data Availability Statement:** The data used to support the findings of this study are included within the article.

**Conflicts of Interest:** The authors declare no conflict of interest.

## References

1. Tang, L.; Li, G.; Li, Z.; Jin, L.; Yang, G. Shear properties and pore structure characteristics of soil–rock mixture under freeze–thaw cycles. *Bull. Eng. Geol. Environ.* **2021**, *80*, 3233–3249. [[CrossRef](#)]
2. Zhang, Y.; Tie, Y.; Wang, L.; Liu, J. CT Scanning of Structural Characteristics of Glacial Till in Moxi River Basin, Sichuan Province. *Appl. Sci.* **2022**, *12*, 3040. [[CrossRef](#)]
3. Tu, G.X.; Huang, R.Q.; Deng, H.; Li, Y.R. Sedimentary Characteristics of the Pleistocene Outwash Accumulation and their Implications for Paleoclimate Change in the Midstream of Dadu River, Southwestern China. *Acta Geol. Sin.-Engl.* **2012**, *86*, 924–931. [[CrossRef](#)]
4. Wang, S.N.; Shi, C.; Xu, W.Y.; Wang, H.L.; Zhu, Q.Z. Numerical direct shear tests for outwash deposits with random structure and composition. *Granul. Matter* **2014**, *16*, 771–783. [[CrossRef](#)]
5. Xie, Y.; Zhang, C.; Yang, J.; Chen, B.; Fu, J.; Zhu, Z. Study on failure characteristics and reinforcement measures of surrounding rock of glacial deposit tunnels based on coarse-grained DEM. *Chin. J. Rock Mech. Eng.* **2021**, *40*, 576–589. [[CrossRef](#)]
6. Latifi, N.; Eisazadeh, A.; Marto, A.; Meehan, C.L. Tropical residual soil stabilization: A powder form material for increasing soil strength. *Constr. Build. Mater.* **2017**, *147*, 827–836. [[CrossRef](#)]
7. Ghadir, P.; Zamanian, M.; Mahbubi-Motlagh, N.; Saberian, M.; Li, J.; Ranjbar, N. Shear strength and life cycle assessment of volcanic ash-based geopolymer and cement stabilized soil: A comparative study. *Transp. Geotech.* **2021**, *31*, 100639. [[CrossRef](#)]
8. Miturski, M.; Gluchowski, A.; Sas, W. Influence of Dispersed Reinforcement on Mechanical Properties of Stabilized Soil. *Materials* **2021**, *14*, 5982. [[CrossRef](#)]
9. Miturski, M.; Sas, W.; Radzevicius, A.; Sadzevicius, R.; Skominas, R.; Stelmaszczyk, M.; Gluchowski, A. Effect of Dispersed Reinforcement on Ultrasonic Pulse Velocity in Stabilized Soil. *Materials* **2021**, *14*, 6951. [[CrossRef](#)]
10. Pu, S.; Zhu, Z.; Huo, W. Evaluation of engineering properties and environmental effect of recycled gypsum stabilized soil in geotechnical engineering: A comprehensive review. *Resour. Conserv. Recycl.* **2021**, *174*, 105780. [[CrossRef](#)]
11. Gu, J.; Lyu, H.; Yang, J.; Zeng, C. Effects of cement content and curing period on geotechnical properties of cement-treated calcareous sands. *Transp. Geotech.* **2022**, *33*, 100732. [[CrossRef](#)]
12. Ikhlef, N.-S.; Ghembaza, M.S.; Dadouch, M. Effect of Treatment with Cement on the Mechanical Characteristics of Silt from Telagh Region of Sidi Belabes, Algeria. *Geotech. Geol. Eng.* **2015**, *33*, 1067–1079. [[CrossRef](#)]
13. Pu, S.; Zhu, Z.; Zhao, L.; Song, W.; Wan, Y.; Huo, W.; Wang, H.; Yao, K.; Hu, L. Microstructural properties and compressive strength of lime or/and cement solidified silt: A multi-scale study. *Bull. Eng. Geol. Environ.* **2020**, *79*, 5141–5159. [[CrossRef](#)]
14. Han, L.; Li, J.; Xue, Q.; Chen, Z.; Zhou, Y.; Poon, C.S. Bacterial-induced mineralization (BIM) for soil solidification and heavy metal stabilization: A critical review. *Sci. Total Environ.* **2020**, *746*, 140967. [[CrossRef](#)]
15. Li, Y.; Li, J.; Cui, J.; Shan, Y.; Niu, Y. Experimental study on calcium carbide residue as a combined activator for coal gangue geopolymer and feasibility for soil stabilization. *Constr. Build. Mater.* **2021**, *312*, 125465. [[CrossRef](#)]
16. Wang, D.; Zhu, J.; He, F. CO<sub>2</sub> carbonation-induced improvement in strength and microstructure of reactive MgO–CaO–fly ash-solidified soils. *Constr. Build. Mater.* **2019**, *229*, 116914. [[CrossRef](#)]
17. Liu, J.; Chen, Z.; Kanungo, D.P.; Song, Z.; Bai, Y.; Wang, Y.; Li, D.; Qian, W. Topsoil reinforcement of sandy slope for preventing erosion using water-based polyurethane soil stabilizer. *Eng. Geol.* **2019**, *252*, 125–135. [[CrossRef](#)]

18. Yang, S.; Liu, W. The Effect of Changing Fly Ash Content on the Modulus of Compression of Stabilized Soil. *Materials* **2019**, *12*, 2925. [[CrossRef](#)]
19. Ma, C.; Zhao, B.; Long, G.; Sang, X.; Xie, Y. Quantitative study on strength development of earth-based construction prepared by organic clay and high-efficiency soil stabilizer. *Constr. Build. Mater.* **2018**, *174*, 520–528. [[CrossRef](#)]
20. Wu, Y.; Shi, K.; Yu, J.; Han, T.; Li, D. Research on Strength Degradation of Soil Solidified by Steel Slag Powder and Cement in Seawater Erosion. *J. Mater. Civ. Eng.* **2020**, *32*, 04020181. [[CrossRef](#)]
21. Wang, S.; Li, X.; Ren, K.; Liu, C. Experimental Research on Steel slag Stabilized Soil and its Application in Subgrade Engineering. *Geotech. Geol. Eng.* **2020**, *38*, 4603–4615. [[CrossRef](#)]
22. Ojuri, O.O.; Adavi, A.A.; Oluwatuyi, O.E. Geotechnical and environmental evaluation of lime–cement stabilized soil–mine tailing mixtures for highway construction. *Transp. Geotech.* **2017**, *10*, 1–12. [[CrossRef](#)]
23. Zhou, S.-Q.; Zhou, D.-W.; Zhang, Y.-F.; Wang, W.-J.; Li, D. Research on the Dynamic Mechanical Properties and Energy Dissipation of Expansive Soil Stabilized by Fly Ash and Lime. *Adv. Mater. Sci. Eng.* **2019**, *2019*, 5809657. [[CrossRef](#)]
24. Inazumi, S.; Intui, S.; Jotisankasa, A.; Chaiprakaikeow, S.; Shinsaka, T. Applicability of mixed solidification material based on inorganic waste as soil stabilizer. *Case Stud. Constr. Mater.* **2020**, *12*, e00305. [[CrossRef](#)]
25. Suo, C.; Fang, P.; Cao, H.; Cao, J.; Liu, K.; Dong, X. Influence and microscopic mechanism of the solid waste-mixture on solidification of Cu<sup>2+</sup>-contaminated soil. *Constr. Build. Mater.* **2021**, *305*, 124651. [[CrossRef](#)]
26. He, J.; Shi, X.-K.; Li, Z.-X.; Zhang, L.; Feng, X.-Y.; Zhou, L.-R. Strength properties of dredged soil at high water content treated with soda residue, carbide slag, and ground granulated blast furnace slag. *Constr. Build. Mater.* **2020**, *242*, 118126. [[CrossRef](#)]
27. Yoobanpot, N.; Jamsawang, P.; Horpibulsuk, S. Strength behavior and microstructural characteristics of soft clay stabilized with cement kiln dust and fly ash residue. *Appl. Clay Sci.* **2017**, *141*, 146–156. [[CrossRef](#)]
28. Katz, L.E.; Rauch, A.F.; Liljestrand, H.M.; Harmon, J.S.; Shaw, K.S.; Albers, H. Mechanisms of Soil Stabilization with Liquid Ionic Stabilizer. *Transp. Res. Rec. : J. Transp. Res. Board* **2001**, *1757*, 50–57. [[CrossRef](#)]
29. Hu, R.; Wang, X.; Liu, H.; Leng, H. Scour Protection of Submarine Pipelines Using Ionic Soil Stabilizer Solidified Soil. *J. Mar. Sci. Eng.* **2022**, *10*, 76. [[CrossRef](#)]
30. Rauch, A.F.; Harmon, J.S.; Katz, L.E.; Liljestrand, H.M. Measured Effects of Liquid Soil Stabilizers on Engineering Properties of Clay. *Transp. Res. Rec. J. Transp. Res. Board* **2002**, *1787*, 33–41. [[CrossRef](#)]
31. Wu, X.-T.; Qi, Y.; Liu, J.-N.; Chen, B. Solidification Effect and Mechanism of Marine Muck Treated with Ionic Soil Stabilizer and Cement. *Minerals* **2021**, *11*, 1268. [[CrossRef](#)]
32. Al-Dakheeli, H.; Arefin, S.; Bulut, R.; Little, D. Effectiveness of ionic stabilization in the mitigation of soil volume change behavior. *Transp. Geotech.* **2021**, *29*, 100573. [[CrossRef](#)]
33. Tingle, J.S.; Newman, J.K.; Larson, S.L.; Weiss, C.A.; Rushing, J.F. Stabilization Mechanisms of Nontraditional Additives. *Transp. Res. Rec. J. Transp. Res. Board* **2007**, *1989-2*, 59–67. [[CrossRef](#)]
34. Wu, X.-T.; Qi, Y.; Chen, B. Solidification effect and mechanism of ionic soil stabilizer applied on high-water-content clay. *Bull. Eng. Geol. Environ.* **2021**, *80*, 8583–8595. [[CrossRef](#)]
35. Lu, X.; Luo, J.; Wan, M.; Zhou, G. Optimization of Ionic Soil Stabilizer Dilution and Understanding the Mechanism in Red Clay Treatment. *Adv. Civ. Eng.* **2021**, *2021*, 5749863. [[CrossRef](#)]
36. Lu, X.S.; Wei, X. Experimental Study on Ionic Soil Stabilizer Reinforcing Red Clay. *Adv. Mater. Res.* **2011**, *183–185*, 1736–1740. [[CrossRef](#)]
37. Lu, X.S.; Xiang, W. Study on Ionic Soil Stabilizer Reinforcing Red Clay of Wuhan. *Adv. Mater. Res.* **2011**, *261–263*, 1129–1133. [[CrossRef](#)]
38. Lu, X.S.; Xiang, W. Experimental Study on Dynamic Characteristics of Ionic Soil Stabilizer Reinforcing Red Clay. *Adv. Mater. Res.* **2011**, *374–377*, 1391–1395. [[CrossRef](#)]
39. Xiang, W.; Cui, D.; Liu, Q.; Lu, X.; Cao, L. Theory and practice of ionic soil stabilizer reinforcing special clay. *J. Earth Sci.* **2010**, *21*, 882–887. [[CrossRef](#)]
40. Zhang, Z.; Zhang, J.; Zhang, H. Effects and Mechanisms of Ionic Soil Stabilizers on Warm Frozen Soil. *Arab. J. Sci. Eng.* **2018**, *43*, 5657–5666. [[CrossRef](#)]
41. Zhang, Z.; Zhang, H.; Zhang, J.; Chai, M. Effectiveness of Ionic Polymer Soil Stabilizers on Warm Frozen Soil. *KSCE J. Civ. Eng.* **2019**, *23*, 2867–2876. [[CrossRef](#)]
42. Huang, W.; Zhang, Y.; Luo, Z.; Wei, X.; Fu, H. Reduction of Clay Hydration by Addition of an Organic Stabilizer. *Clays Clay Miner.* **2021**, *69*, 489–499. [[CrossRef](#)]
43. Huang, W.; Feng, Z.; Fu, H.; Xiang, W.; Hua, M. Evolution of Pore Characteristics for Bentonite Modified by an Ionic Soil Stabilizer during Hydration Processes. *Adsorpt. Sci. Technol.* **2021**, *2021*, 7777091. [[CrossRef](#)]
44. Wu, X.-T.; Sun, J.-S.; Qi, Y.; Chen, B. Pore and compression characteristics of clay solidified by ionic soil stabilizer. *Bull. Eng. Geol. Environ.* **2021**, *80*, 5003–5019. [[CrossRef](#)]
45. He, S.; Yu, X.; Banerjee, A.; Puppala, A.J. Expansive Soil Treatment with Liquid Ionic Soil Stabilizer. *Transp. Res. Rec. J. Transp. Res. Board* **2018**, *2672*, 185–194. [[CrossRef](#)]
46. Arefin, S.; Al-Dakheeli, H.; Bulut, R. Stabilization of expansive soils using ionic stabilizer. *Bull. Eng. Geol. Environ.* **2021**, *80*, 4025–4033. [[CrossRef](#)]

47. Li, J.-D.; Wang, X.; Zhang, Y.-J.; Jiang, D.-J.; Liu, D.-R.; Wang, J.-L. Study on strength characteristics and mechanism of loess stabilized by F1 ionic soil stabilizer. *Arab. J. Geosci.* **2021**, *14*, 1162. [[CrossRef](#)]
48. Sun, P.; Zhu, J.; Zhao, B.; Zhang, X.; Cao, H.; Tian, M.; Han, M.; Liu, W. Study on the Mechanism of Ionic Stabilizers on Shale Gas Reservoir Mechanics in Northwestern Hunan. *Energies* **2019**, *12*, 2453. [[CrossRef](#)]
49. Lin, Z.-X.; Liu, L.-M.; Liu, L.-W. Validation of the solidifying soil process using laser-induced breakdown spectroscopy. *Opt. Laser Technol.* **2016**, *83*, 13–15. [[CrossRef](#)]
50. Gautam, S.; Hoyos, L.R.; He, S.; Prabakar, S.; Yu, X. Chemical Treatment of a Highly Expansive Clay Using a Liquid Ionic Soil Stabilizer. *Geotech. Geol. Eng.* **2020**, *38*, 4981–4993. [[CrossRef](#)]
51. JTG 3430-2020. *Test Methods of Soils for Highway Engineering*; People's Communications Press: Beijing, China, 2020. (In Chinese)
52. Li, G.-Y.; Hou, X.; Mu, Y.-H.; Ma, W.; Wang, F.; Zhou, Y.; Mao, Y.-C. Engineering properties of loess stabilized by a type of eco-material, calcium lignosulfonate. *Arab. J. Geosci.* **2019**, *12*, 700. [[CrossRef](#)]
53. Zhao, H.; Ge, L.; Petry, T.M.; Sun, Y.-Z. Effects of chemical stabilizers on an expansive clay. *KSCE J. Civ. Eng.* **2013**, *18*, 1009–1017. [[CrossRef](#)]